Dr. Junifa Layla Sihombing, M.Sc_4

by Dr. Junifa Layla Sihombing

Submission date: 20-Feb-2023 02:39PM (UTC+0700)
Submission ID: 2018686201
File name: Manuscript-revised_fix.pdf (2.34M)
Word count: 9265
Character count: 48792

Effective Hydrodeoxygenation Bio-Oil via Natural Zeolite Supported Transition Metal Oxide Catalyst

Junifa Layla Sihombing[1*], *Herlinawati Herlinawati*[1], *Ahmad Nasir Pulungan*[1], *Lisnawaty Simatupang*[1], *Rahayu Rahayu*[1], *Ary Anggara Wibowo*[2]

[1]Department of Chemistry, Faculty of Mathematics and Natural Sciences, Universitas Negeri Medan, Jl. Willem Iskandar Pasar V Medan Estate, Medan 20221, Indonesia

[2]School of Engineering, College of Engineering and Computer Science, The Australian National University, North Road, 2601, Australian Capital Territory, Australia

[*]**Corresponding Author**: junifalaylasihombing@unimed.ac.id

Abstract

Bio-oil from biomass pyrolysis is promising to be used as a sustainable biofuel and high-value-added chemical. However, the presence of high acid, water, and oxygenate causes corrosive properties, low higher heating value (HHV), and instability of the bio-oil component. Therefore, refining the bio-oil is essential to improve its quality. In this study, we introduced natural zeolite (HZ) impregnated with transition metal oxide (TMO) to refine the bio-oil using the hydrodeoxygenation method (HDO) at various catalyst ratios and temperatures. We find that ZnO/HZ 5% wt. shows the best catalytic performance, with the conversion of organic phase reaching ~ 50%. The refined bio-oil from Fe_2O_3, ZnO, and CuO has high-quality physicochemical properties with carbon, oxygen, water level, and HHV values are 37-52%, 40-53%, 8-27%, and 17-21 MJ/kg, respectively. This result represents a high catalytic performance for the hydrodeoxygenation process of bio-oil using natural zeolite-based transition metal oxide for better and low-cost biofuel production.

Keywords: *hydrodeoxygenation, upgraded bio-oil, metal oxide catalyst, zeolite support*

1. Introduction

High dependencies on fossil fuels have a significant impact on climate change which triggers an interest in finding alternative energy that is cleaner and more sustainable. Biofuels are one of the sustainable energies that have the potential to reduce CO_2 emissions. It contributes ~6% of the world's energy mix [1]. Biofuel can be produced from biomass pyrolysis as a form of bio-oil. However, bio-oil has poor physiochemical properties (e.g., high acid, oxygenate, and water level), leading to low quality and performance. Hydrodeoxygenation (HDO) and catalytic cracking are the most common techniques to improve bio-oil quality [2–7]. Removing oxygen from bio-oil through catalytic cracking can be carried out at atmospheric pressure without hydrogen. However, this process has not been effectively used on a larger scale due to high coke formation and catalyst deactivation [8,9]. HDO is more developed because it includes various reaction pathways such as decarboxylation, hydrogenation, demethylation, demethoxylation, and direct deoxygenation. HDO-assisted hydrogen and heterogeneous catalyst are efeffectively reduce double bonds and/or eliminating oxygen atoms from a compound. The oxygen is released mainly in the form of H_2O, CO_2, and CO. Moreover, the HDO process is reported to have several advantages over catalytic cracking due to higher organic phase and lower coke product. [10,11]

Bio-oil refining through the HDO process by using a noble metal [12], transition metal [13,14], carbon, and zeolite [15] – catalysts, are widely researched. Transition metal catalysts have a high catalytic performance and low cost. It exhibits a specific reaction pathway and selectivity for a particular compound. An active metal group such as Ruthenium (Ru), palladium (Pd), platinum (Pt), and nickel (Ni) tends to form a hydrogenation process. In contrast, exophilic groups such as iron (Fe), tungsten (W), rhenium (Re), and molybdenum (Mo) have a higher affinity for oxygen atoms and advantageous in the deoxygenation pathway [16]. However, these metals have a relatively small surface area and are easy to sinter

forming aggregations that reduce catalytic performance. On the other hand, zeolite has a large surface area, good thermal stability at high temperatures, and contains Bronsted and Lewis active sites that can be modified by acidity. Further, zeolite can act as a support material by trapped the metals into their frameworks. A support material with suitable acidity can significantly increase the production of liquid hydrocarbons by increasing the dehydration/hydrogenation of the intermediate product. The relatively large pore size of the modified zeolite allows the reactants and intermediates to overcome the limitations of diffusion and adsorptioan at metal active site [17,18]. Therefore, combining metal and zeolite as catalysts results in a synergistic role between metal functions and acid sites in facilitating various reaction pathways, both hydrogenation, and deoxygenation.

Gea et al. [19] perform HDO bio-oil using a natural zeolite catalyst impregnated with nickel metal at a reaction temperature of 250 °C for 2 hours. This catalyst shows good performance in stabilizing raw bio-oil by increasing HHV (up to 21 MJ/kg), decreasing water content (13%), and improving deoxygenation (88%). Moreover, Xu et al. [18] suggest that Zn to HZSM-5 and HY could inhibit biochar production and increase the production of organic bio-oils and aromatic amines. When using a ZnO/HZSM-5 catalyst, the carbon yields of organic bio-oils and aromatic amines reach 9.8% and 5.6%, which is much higher than that of HZSM-5 and ZnO/HY catalyst showing the carbon yield of organic bio-oil and aromatic amines reach 5.2% and 4.5%, respectively. Further, Choo et al. [19] present that the presence of transition metal oxides such as NiO, ZnO, CuO, CoO, and MnO on zeolite Y change the strength and distribution between Bronsted and Lewis acidity, thus increasing triolein conversion and reducing the intermediate reaction product. Despite the use of transition metal oxide on synthetic zeolite, the study on natural zeolite as a supported catalyst is limited.

In this research, we employ natural zeolite (HZ) as a supported catalyst for the hydrodeoxygenation process of bio-oil refining. First, we introduce transition metal oxide

(Fe_2O_3, CuO, and ZnO) embedded into active sites of natural zeolite to produce Fe_2O_3/HZ, CuO/HZ, and ZnO/HZ catalysts. The catalyst characteristic is measured by X-ray diffraction (XRD), scanning electron microscope (SEM) equipped with the ability of energy dispersive spectroscopy (EDX), and gas adsorption analyzer. Next, we test their catalytic performance in the bio-oil hydrodeoxygenation process in a fixed-bed reactor at various temperatures and ratios of the catalyst to obtain optimal results. Then, the upgraded bio-oil product's physicochemical (viscosity, elemental, compound, density, HHV, and acidity) is analyzed and compared with the untreated bio-oil. The exploration of novel natural zeolite impregnated with transition metal oxide (TMO/HZ) could contribute to the biofuel and catalyst community finding high-performance and low-cost catalysts.

2. Material and Methods

The materials used in this research are bio-oil from coconut shell pyrolysis, distilled water (DI), and natural zeolite from CV. Bratachem, Indonesia, $Zn(NO_3)_2.4H_2O$ (p.a), $FeCl_3.6H_2O$ (p.a), $CuSO_4.5H_2O$ (p.a), HCl (p.a) from Merck (Darmstadt, Germany), hydrogen, oxygen and nitrogen gases from PT. Aneka Gas (Medan, Indonesia).

2.1 Preparation of ZnO/H-Z, Fe_2O_3/H-Z, and CuO/H-Z catalysts

Zeolite is activated using 5M HCl following the procedure reported by Gea et al. [20]. The acid-activated zeolites are labeled H-Z. The wet impregnation method carries metal loading on the active zeolite [21]. 100 g of zeolite is mixed with a precursor salt containing 1% (wt.) metal dissolved in 100 mL of distilled water. This mixture is refluxed, stirred at 80 °C for 5 hours, and dried. Next, the dried mix is calcinated at 500 °C for 2 hours with N_2 gas flow and oxidized under the same conditions using O_2 gas. The final product is Fe_2O_3/H-Z, ZnO/H-Z, and CuO/H-Z catalysts.

2.2 Catalyst Characterization

The crystallinity properties of the catalyst are analyzed by X-Ray Diffractometer (XRD Shimadzu 6100) Cu Kα (λ = 1.54184) radiation at 40kV and 30 mA in the area 2θ= 7.00 – 70.00°. The catalyst's surface morphology, elemental analysis, and mapping are analyzed using a Zeiss EPOMH 10Zss SEM equipped with Energy Dispersion X-Ray Spectroscopy (EDX). The nitrogen gas adsorption-desorption isotherm analysis is carried out with the Gas Sorption Analyzer (NOVA 1200e) Quantachrome instrument at 77 K. The specific surface area is analyzed by the Brunauer-Emmett-Teller (BET) method. Meanwhile, the volume and pore diameter is based on the Barret-Joyner-Halenda (BJH) model.

2.3 Hydrodeoxygenation of Bio-oil

The upgrading process of bio-oil using the Hydrodeoxygenation method is carried out in a fixed-bed reactor with the metal oxide catalyst impregnated on an active natural zeolite. The reactor where the reaction takes place has a diameter of 5.5 cm with a height of 25 cm, a catalyst vessel with a diameter of 4.8 cm and a height of 3.5 cm, while the furnace has a diameter of 40 cm and a height of 39 cm. The reactor scheme used is shown in **Figure 1**. In mild HDO, the reaction occurs at a temperature of 250 °C and a pressure of 1 atm for 2 hours. The catalyst that shows the best catalytic activity is optimized at temperatures 250, 275, and 300 °C, and the catalyst ratio at 2.5, 5.0, 7.5, and 10 % (wt.). The steam resulting from the reaction is passed through a silicone hose and passes through a condenser, where the liquid product consisting of aqueous and organic phases is collected. The aqueous phase and the organic phase were separated and then the mass proportion was calculated from the initial sample mass. During the reaction process, non-condensable gas is also generated and coke is formed on the surface of the catalyst.The product of the reaction is calculated as follows [22]:

$$Y_{product}(\%) = \frac{M_{product\ (g)}}{M_{raw\ bio-oil\ (g)}} x\ 100 \qquad (1)$$

$$Y_{gas}(\%) = 100 - [Y_{aqueous\ phase} + Y_{organic\ phase} + Y_{coke}] \quad (2)$$

Where $Y_{product}$ and $M_{product}$ are the yield (liquid phase, organic phase, and coke) and mass of the products, respectively.

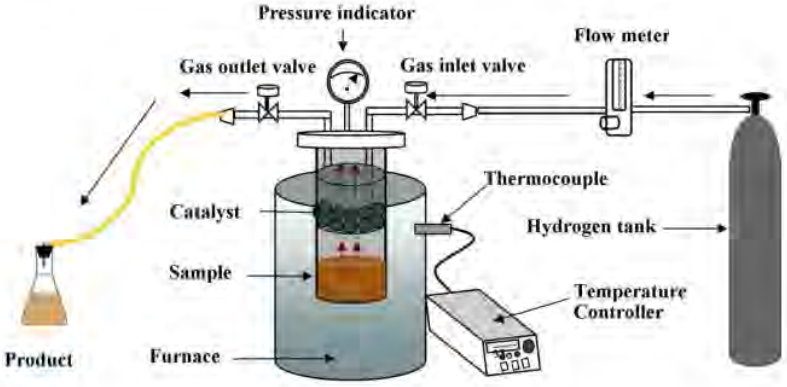

Figure 1. Schematic of hydrodeoxygenation process with fixed-bed reactor system

2.4 HDO Product Analysis

Physicochemical properties and components of untreated and treated (HDO) bio-oil products are characterized by using Ostwald Viscometer for viscosity, CHN Analyzer LECO-CHN 628 for elemental analysis, pycnometer for density, titration method for acid number. Analysis of compound composition using GC-MS Model QP2010 (Shimadzu) with RTx-5MS capillary column (5% diphenyl- 95% dimethylpolysiloxane crosslinks) with a film thickness of 30 m x 0.25 mm x 0.25 μm under the following conditions: split less inject mode at 300 °C using He as carrier gas and column flow in 0.54 mL/min. HHV is calculated by using the formula reported by [23]. The degree of deoxygenation (DOD) was estimated based on the molar ratio (MO) of raw bio-oil and upgraded products. MO is the atomic ratio of O/C obtained from the molar ratio of O and C based on elemental analysis.

$$DOD(\%) = \frac{MO_{raw\ bio-oil} - MO_{upgraded\ product}}{MO_{raw\ bio-oil}} x\ 100 \quad (3)$$

3. Results and Discussion

3.1 Crystallinity Properties

The crystallinity properties of the material are analyzed using X-ray diffraction. The obtained diffractogram is compared with the pattern between the active natural zeolite and the metal oxide-impregnated zeolite, as shown in **Figure 2**. The resulting diffractogram pattern consists of several characteristic peaks with a certain intensity. High and sharp peaks indicate higher crystallinity [24]. Peak characteristics for natural zeolite are observed in the range of 2θ = 9-30° for mordenite and clinoptilolite. The mordenite mineral type is shown in 2θ = 9.61°, 19.48°, 25.53°, 27.57°, and 30.76° in line with JCPDS no. 11-0155. The clinoptilolite mineral type can be seen in 2θ = 13.35°, 21.93°, 23.31°, 26.42°, and 29.84°, similar to JCPDS no 25-1349. The presence of these peaks with the same pattern in each zeolite indicates that the treatment that has been given during the impregnation and calcination processes does not damage the mineral structure in general.

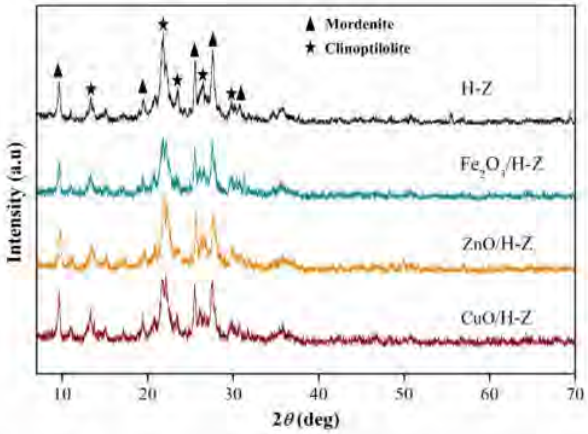

Figure 2. X-ray diffraction of natural zeolite impregnated with transition metal oxide.

The magnitude of the intensity of the peaks possessed by the zeolite can indicate the degree of relative crystallinity of the zeolite (**Table 1**). The degree of crystallinity of the

active zeolite decreases after the immobilization of the metal oxide [25]. The decrease in peak intensity after the impregnation process suggests that the embedded metal oxides in the zeolite have partially covered the crystal side of the zeolite. However, the typical peaks of metal oxides Fe_2O_3 pada 33.1°, 35.6°, and 54.0° (JCPDS 01-072-0469), ZnO pada 35.45°, 39.84°, and 43.36° (JCPDS 01-1316), and CuO pada 39.97°, 42.12°, and 57.01° (JCPDS 45-0937) do not appear on the diffractogram because only 1% (wt.) of metal mass is carried in the impregnation process. Moreover, the metals are successfully dispersed into the zeolite pores[26–28], or well distributed as non-crystalline phases [29]. The metal's presence in zeolites can be seen in **Figure 4**.

Table 1. Comparison of the degree of crystallinity of the catalyst

Catalis	Degree of crystallinity (%)
H-Z	84.9
Fe_2O_3/H-Z	79.1
ZnO/H-Z	74.4
CuO/H-Z	69.9

1

3.2 Surface Morphology

Figure 3. shows the observed surface morphology of the catalyst at a magnification of 1000 times. The activated natural zeolite exhibits a denser surface and aggregated particles with various particle sizes. Meanwhile, the zeolite modified with metal oxides shows a looser surface morphology, but there are also larger particle clumps, especially in the Fe_2O_3/H-Z and CuO/H-Z catalysts with large particle sizes. This can occur due to metal sintering embedded on the surface of the zeolite so that the particles form larger aggregates. However, the surface morphology of the ZnO/H-Z catalyst looks more homogeneous particle sizes.

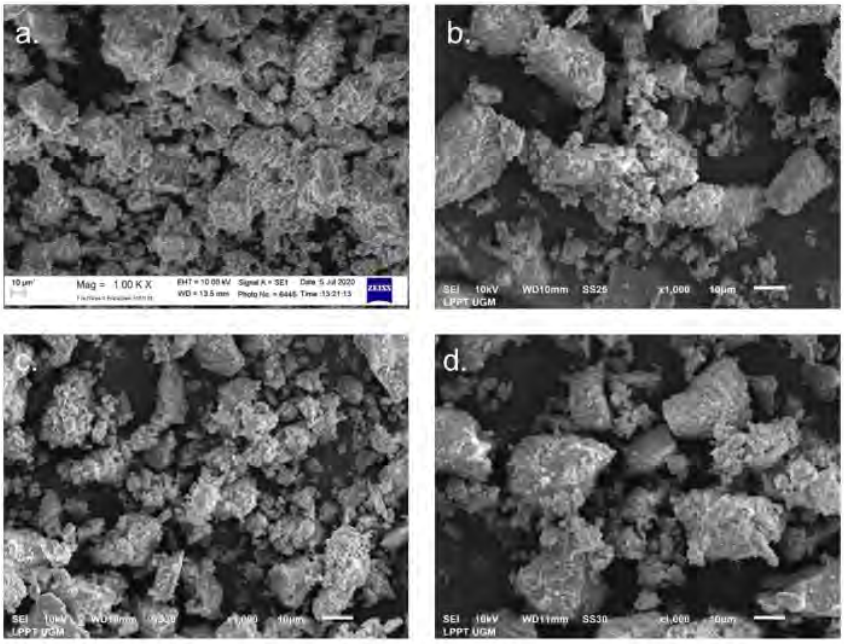

Figure 3. Surface morphology of H-Z, Fe_2O_3/H-Z, ZnO/H-Z, and CuO/H-Z catalysts at 1000x magnification

The components contained in the catalyst are summarized in **Table 2**. Zeolite modified with metal oxides decreased Si and Al levels and increased O levels compared to activated natural zeolites. A reduction in Si and Al levels, along with a decrease in the Si/Al ratio, indicates a change that occurred during the impregnation, calcination, as well as oxidation process. Calcination at high temperatures can cause part of the skeleton to collapse, releasing Si and Al from the zeolite framework [30]. The high value of the Si/Al ratio is also linear to the high degree of crystallinity. Meanwhile, the O content increases significantly, almost threefold, due to the presence of metal oxides. Metals Fe, Zn, Cu attached to the zeolite are detected at 1.27, 1.30, and 2.32 wt%, respectively.

Table 2. Composition and ratio of Si/Al on H-Z, Fe_2O_3/H-Z, ZnO/H-Z, andCuO/H-Z catalysts

Composition (Mass%)	H-Z	Fe_2O_3/H-Z	ZnO/H-Z	CuO/H-Z
Si	57.7	28.9	32.5	30.4
Al	7.41	4.17	4.90	5.35
O	19.5	50.8	48.4	42.3
Fe	-	1.27	-	-
Zn	-	-	1.30	-
Cu	-	-	-	2.32
Impurities	15.4	14.8	12.9	19.6
Si/Al	7.79	6.94	6.63	5.69

The distribution of the elements on the zeolite can be identified by SEM-Mapping, as shown in **Figure 4**. A specific color represents each element. The brighter the color, the more these elements are distributed on the surface of the zeolite. All the catalysts show a color dominated by red, green, and yellow with a slight blue tint (**Figure 4**). This is in line with the data on catalyst composition by EDX analysis, where the most significant compositions are O (green) 42-50 wt%, Si (red) 28-32 wt%, and Al (yellow) 4-5 wt%. Meanwhile, Fe, Zn, and Cu metals are shown in blue and are not too dominant because they only have a small percentage. A scattered blue color indicates that the metal distribution occurs evenly on the zeolite surface.

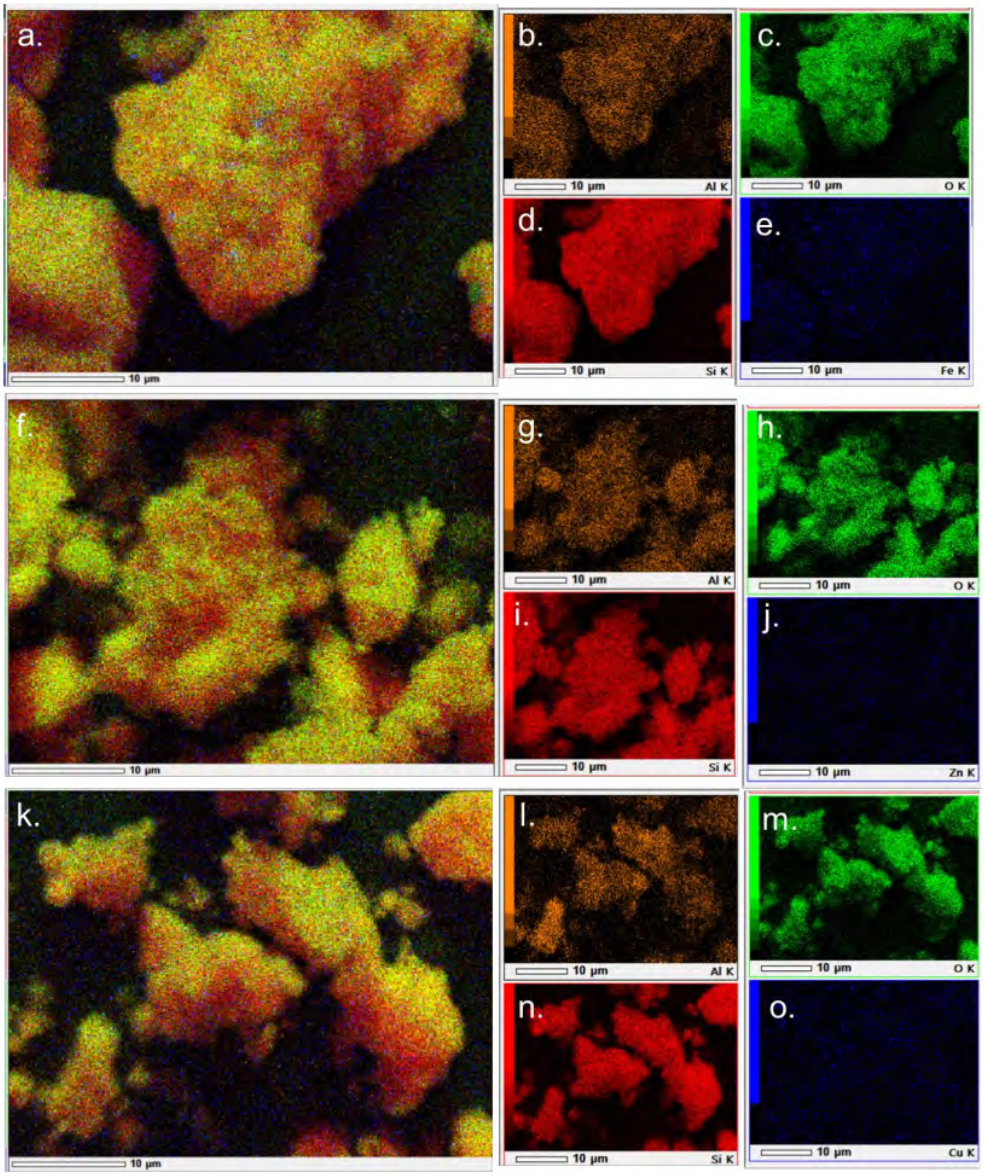

Figure 4. SEM-EDX elemental mapping of the catalyst (a-e) Fe_2O_3/H-Z, (f-j) ZnO/H-Z; and (k-o) CuO/H-Z. The distribution of elements shows different color for aluminum with orange color, oxygen with green color, silicon with red color, and iron, zinc, and copper with blue color.

3.3 N_2 Gas Sorption Analysis

The graph of the adsorption-desorption isotherm of each catalyst is shown in **Figure 5**. The catalyst exhibits a type IV N_2 adsorption-desorption isotherm based on the IUPAC classification with low adsorption at relatively low pressures associated with micropores [31]. Meanwhile, the presence of an H3-type hysteresis loop at relatively high pressure is the result of the adsorption and desorption of N_2 in the mesopores [32,33].

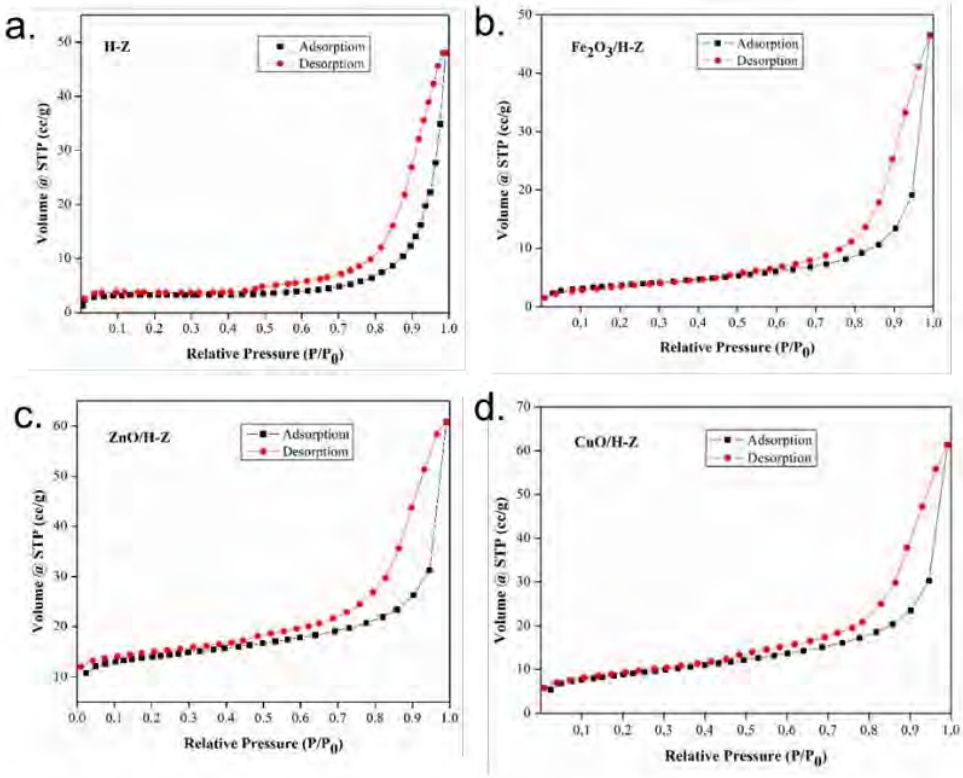

Figure 5. Graph of N_2 gas adsorption-desorption isotherm on H-Z, Fe_2O_3/H-Z, ZnO/H-Z, and CuO/H-Z catalysts

Further analysis is carried out to determine the effect of the metal oxide loading process on the catalyst characteristics, including surface area, total volume, and pore diameter. The BET method calculates the surface area, while the pore volume and pore size are analyzed from the adsorption band using the BJH method. The results of the measurement of the surface area, pore volume, and pore diameter of each catalyst are summarized in **Table 3**.

Table 3. Surface area, pore volume, and pore diameter of the catalyst

Catalyst	Surface area (m^2/g)	Pore volume (cc/g)	Pore diameter (nm)
H-Z	12.3	0.075	3.63
Fe_2O_3/H-Z	12.9	0.070	3.13
ZnO/H-Z	50.3	0.077	3.33
CuO/H-Z	30.7	0.086	3.10

The data in **Table 3** shows that the modification of zeolite with metal oxide loading causes an increase in the surface area, pore size, and pore volume. The ZnO/H-Z catalyst has the largest surface area, but the CuO/H-Z catalyst has the largest pore volume and average pore radius. This change occurs due to the activation process, both acid activation and calcination and metal impregnation processes that impact the surface morphology of the zeolite. These changes are caused by the opening of the active zeolite pores, which are initially still covered by impurities. During the calcination process, impurity molecules such as water and gas, which are chemically bonded to the surface of the zeolite, evaporate to form an empty space (see schematics in **Figure 6**). The results of the analysis also show that the specific surface area increases after metal impregnation is carried out. The entry of metal resulted in the expansion of the space between the zeolite layers so that a good pore system is

formed, and the surface area is larger. With the increase in surface area, the absorption process will be even greater [34]. According to Widayatno et al. small Cu species may enter the zeolite channel and generate new surface area within the channel by increasing the surface roughness. Meanwhile, Cu species loaded on the outer surface of the zeolite can generate new mesoporous surface areas [35]. The comparison of the pore size distribution for each catalyst is shown in **Figure 7**. The pore size distribution for the metal oxide impregnated catalyst shows dominance in the relatively equal radius size range from 15-100 Å (1.5-10 nm).

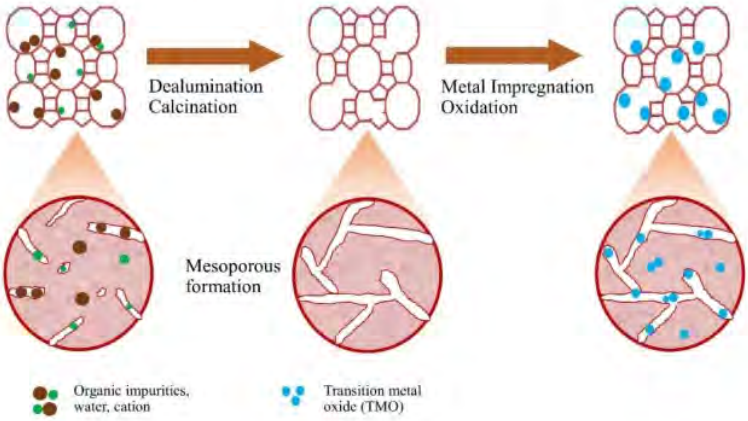

Figure 6. Schematics of impregnated TMO in natural zeolite

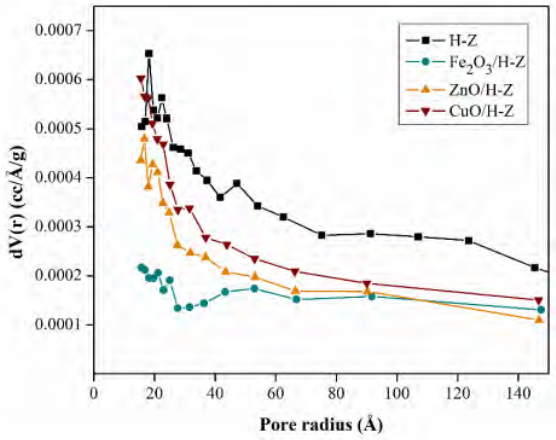

Figure 7. Comparison of the pore size distribution of H-Z, Fe_2O_3/H-Z, ZnO/H-Z, and CuO/H-Z catalysts

3.4 Bio-oil Hydrodeoxygenation

The distribution of the products resulting from the hydrodeoxygenation of bio-oil with Fe_2O_3/H-Z, CuO/H-Z, and ZnO/H-Z catalysts is shown in **Figure 8**. Based on the data in the table, the bio-oil catalyzed by Fe_2O_3/H-Z produces more organic, gas, and coke phases than other catalysts. Meanwhile, the bio-oil catalyzed by ZnO/H-Z and CuO/H-Z has the most aqueous phase but less coke, gas, and organic. A lower organic phase yield is associated with more efficient deoxygenation results [36]. Deoxygenation reaction produces water as a by-product so that large amounts of water are released along with the decrease in the mass of the organic phase. Huang et al. [37] state that Fe_2O_3 contributes to increased gas yield but decreases liquid bio-oil and bio-char product yield. Fe_2O_3 can encourage the formation of CO and H_2 but inhibit the formation of CH_4 [37]. Meanwhile, Konadu et al.[38] performed hydrodeoxygenation of guaiacol using Cu catalyst and reported that Cu (111) plays a selective role in the transformation of guaiacol into catechol through the direct demethylation pathway.

Each catalyst's difference in product distribution is due to the characteristics of each catalyst, such as surface area and pore volume. Fe_2O_3/H-Z has a smaller surface area and pore volume than ZnO/H-Z and CuO/H-Z. This difference provides a significant gap in the selectivity of the liquid product, where the larger surface area and pores can support better diffusion and adsorption of reactants, which causes more reactant molecules to bind to the active site of the zeolite to undergo a catalytic process.

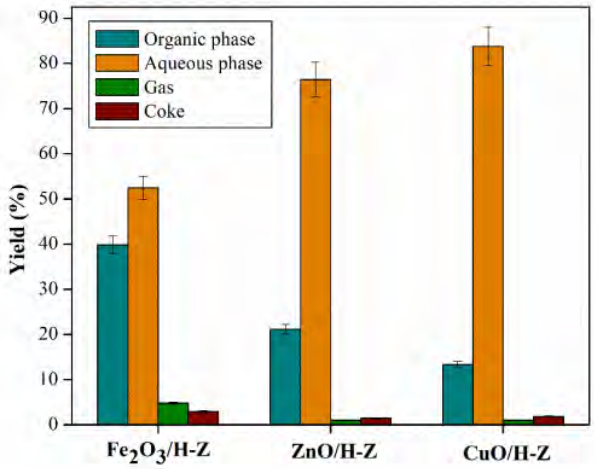

Figure 8. Product distribution of upgraded bio-oil catalyzed by Fe_2O_3/H-Z, ZnO/H-Z, and CuO/H-Z (catalyst loading of 2.5 wt.%, temperature 250 °C for 2 hours)

3.5 Physicochemical properties

The product analyzed in this study is the organic phase because it contains rich organic compounds such as phenols and their derivatives, as well as aromatic compounds which have the potential for fuel applications. While the aqueous phase contains more water and acids which reduce its quality as fuel. Analysis of physicochemical properties of bio-oil products is carried out including elementary content, HHV, viscosity, acid number, and analysis of compound content using GC-MS. The physicochemical properties are summarized in **Table 4**.

Table 4. Physicochemical properties of pyrolysis and upgraded bio-oil

Properties	Raw bio-oil	Fe_2O_3/H-Z	ZnO/H-Z	CuO/H-Z
Elemental analysis (wt%)				
C	14.3	37.9	51.7	51.8
H	9.88	7.77	6.84	6.86

N	0.55	0.01	1.02	1.11
O[a]	75.8	53.8	40.5	40.2
Water content (%)	68.6	27.0	10.1	8.30
Density (g/cm^3)	1.02	1.11	1.18	1.23
HHV (MJ/kg)[b]	12.5	17.7	20.9	20.9
Viscosity (cP)	0.98	2.31	2.52	3.13
Acid number (mg NaOH/g oil)	171	139	166	118
H/C	8.29	2.46	1.59	1.59
O/C	3.98	1.06	0.59	0.58
DOD (%)	-	73.4	85.2	85.4

[a]calculated by the difference

[b]High heating value is calculated by using the following formula reported in Sheng and Azevedo [23]:

HHV (MJ/ kg) = -1.3675 + (0.3137 C) + (0.7009 H) + (0.0318 O)

Bio-oil catalyzed by ZnO/H-Z and CuO/H-Z catalysts has less oxygen and higher carbon content than bio-oil catalyzed by Fe_2O_3/H-Z. A smaller molar O/C and an increased H/C ratio of HDO bio-oil indicates a direct deoxygenation and hydrogenation reaction pathway[39]. In this study, the molar ratios of O/C and H/C both decreased. It suggests the deoxygenation pathway releasing water and acid is the dominant pathway in the HDO bio-oil reaction with a metal oxide-embedded activated zeolite catalyst [36,40]. ZnO/H-Z and CuO/H-Z catalysts have DOD ranging ~85%. Product viscosity and HHV also increase as a result of reduced water content in bio-oil [41]. However, the acid number is still high (118-166 mg NaOH/g oil) due to the high acid content in bio-oil. This high acidity level is mainly determined by phenolic compounds, which are measured as weak acids by the TAN method [42].

ZnO/H-Z catalyst has a larger surface area, pore volume, and pore diameter and shows better selectivity for the water fraction. This is related to the character of the catalyst with a

larger surface area and pores, facilitating more reaction pathways. The deoxygenation pathway can occur more by producing water as a by-product [43]. Zn can selectively break C–O bonds in various lignin molecules under relatively mild reaction conditions [44–46]. With more oxygen coming out as water molecules, the bio-oil product catalyzed by the ZnO/H-Z catalyst has a higher viscosity and HHV value of 2.52 cP and 20.9 MJ/Kg, respectively. Meanwhile, the bio-oil catalyzed by the Fe_2O_3/H-Z catalyst tends to have a high oxygen content, and the HHV value only increases slightly compared to the pyrolysis bio-oil.

3.6 Compounds in Bio-oil

GC-MS are carried out to examine molecule content in the bio-oil and HDO products, which is summarized in **Figure 9**.

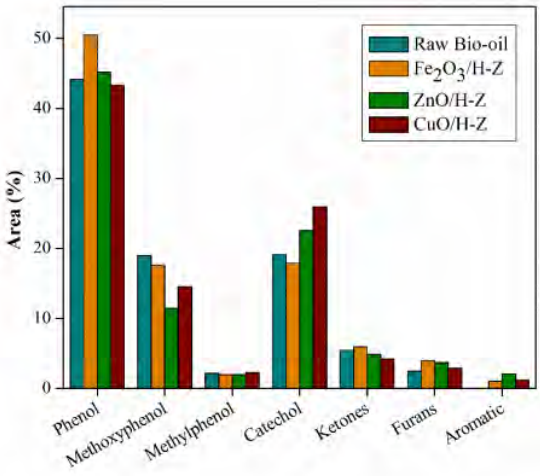

Figure 9. Composition of compounds in raw bio-oil and organic phase products catalyzed by Fe_2O_3/H-Z, ZnO/H-Z, and CuO/H-Z (catalyst loading of 2.5 wt%, temperature 250 °C for 2 hours)

GC-MS diffractogram of bio-oil reveals the composition of ketones, phenols, methyl phenols, methoxyphenyl, and furans. Compounds in bio-oil are dominated by lignin derivatives such as

phenol, guaiacol, syringol, and pyrocatechol compounds, as well as cellulose derivatives such as aldehydes, ketones, furan derivatives, and phenols [47]. Furfural compounds during the HDO process can undergo hydrogenation to produce furfuryl alcohol compounds which are further converted to tetrahydrofurfuryl alcohol, ketones, and other open ring products [48]. This can be proven by the decrease in the percent area of furan compounds and the increase in the percent area of ketone compounds in the HDO bio-oil product of each catalyst.

The phenol content generally increased after the HDO process with all catalysts, especially with Fe_2O_3/H-Z and ZnO/H-Z catalysts. Meanwhile, the methoxy phenol group of compounds decreased, including syringol and guaiacol [49]. However, intermediate compounds such as catechol and pyrocatechol compounds have increased. Catechol is formed as an intermediate in the conversion of Phenol-2 methoxy to cyclohexanone, produced by the cleavage of the methyl and methoxy groups from guaiacol and syringol, respectively [46]. In this case, the increase in certain compounds related to the conversion of other compounds, such as reduced syringol may undergo a demethoxylation reaction to guaiacol, which then undergoes demethoxylation again to produce more stable phenolic compounds [50,51]. Meanwhile, another methoxyphenol group, guaiacol, can go through several reaction pathways, (i) through demethoxylation where the methoxy group is cleaved to produce phenol; (ii) through the demethylation pathway, where the C-O bond cleaves from methoxy and releases it as CH_4 to produce catechol intermediates. Catechol can be deoxygenated to produce phenol, (iii) deoxygenated to cresol which can then be demethylated to produce phenol [52–54]. The various reaction pathways that lead to the formation of phenol compounds cause by the high percentage of the area owned by phenol. Furthermore, through the direct deoxygenation pathway, phenol breaks the $C_{aromatic}$ -OH bond to form benzene as an aromatic hydrocarbon product [55,56]. Some schematics of the possible reaction pathways during the HDO bio-oil process are shown in **Figure 10**.

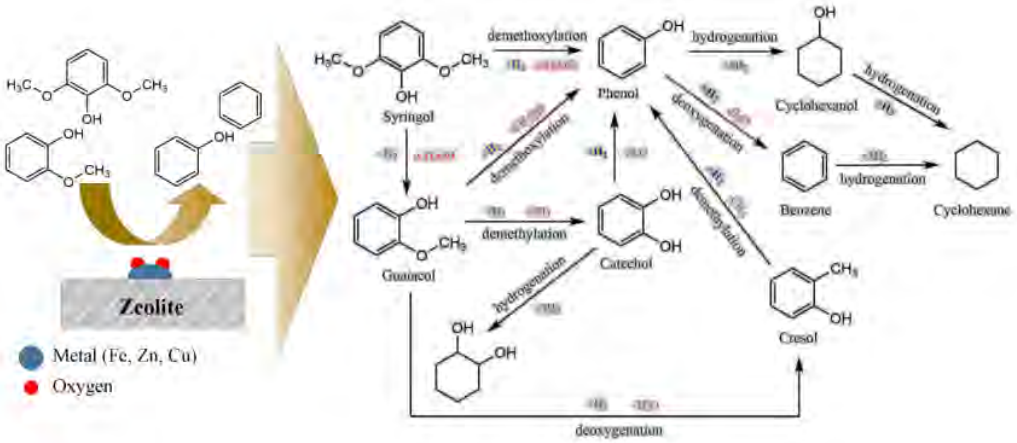

Figure 10. Possible reaction pathways in the bio-oil component HDO

The acidic sites in the catalyst promote C-O cleavage, while metal sites influence the hydrogenation of the benzene ring. Metals activate H_2, while oxygenating Brønsted acid sites activate compounds. The Brønsted acid site interacts with the oxygen atom of the oxy compound, whereas H_2 is started by metals and causes C-O bond cleavage instead of C-C bond cleavage [57]. Furthermore, the redox-active components of metals play an important role in HDO reactions because these metal sites can facilitate both hydrogenation and dehydrogenation reactions [58].

The active site of Fe is reported to have good ability in the direct deoxygenation pathway [59,60], but in this study, the characteristics of the Fe_2O_3/H-Z catalyst were not superior to the material aspects of the ZnO/H-Z catalyst. Meanwhile, the presence of copper in the catalyst is essential for the hydrogenation reaction, which can increase the conversion yield of bio-oil products [61]. Moreover, Cu catalysts can facilitate dehydration reactions by forming Cu-alkoxide species [62]. In addition, ZnO provided suitable acidity to reduce the C-O hydrogenolysis reactivity [63]. In the metal oxide catalytic mechanism, lattice oxygen reacts with H_2, and an oxygen vacancy is created, which is further filled by oxygen from the oxy compound. Then the intermediate compound undergoes C-O cleavage and forms the final

product. He and Wang [64] reported that the order of metal-oxygen bonds from the stronger is Zn > Fe > Cu. This metal-oxygen bond will affect the course of the reaction during HDO. When the metal-oxygen bond is too weak, it will be difficult for the catalyst to abstract oxygen from the oxy compound. Still, when the metal-oxygen bond is too strong, it is challenging to create a surface vacancy to adsorb the oxy-compound [65].

3.7 Effect of temperature

The ZnO/H-Z catalyst is further tested for its activity to catalyze bio-oil at higher temperatures, 275 and 300 °C. The distribution of the resulting product is shown in **Figure 11**. Organic phase and gas increase when the temperature is increased to 275 °C and then decrease when the temperature reaches 300 °C. On the other hand, the aqueous phase and coke drop at 275 °C and then increase at 300 °C. This difference in product distribution trends at each temperature indicates that temperature affects the yield [66]. Meanwhile, more gas content occurs at a temperature of 275 °C, suggesting that increasing temperature promotes gasification reactions or hydrocracking of bio-oil to convert organic compounds into gaseous products [67]. In a previous study, Cheng et al. [68] tested out HDO bio-oil at temperatures of 250, 300, 350, and 400 °C and reported that the main compositions of gaseous products formed during HDO were CO_2, H_2, CO, N_2, CH_4, and C_2H_6. Meanwhile, at the highest temperature at 300 °C, the organic phase was reduced significantly and tended to promote coke formation on the catalyst surface, reducing the catalytic activity. The increase in coke at high temperatures can be caused by polymerization reactions and condensation of bio-oil components [69]. The organic phase is then analyzed for its components using GC-MS, and the resulting compounds are summarized in **Figure 11a**.

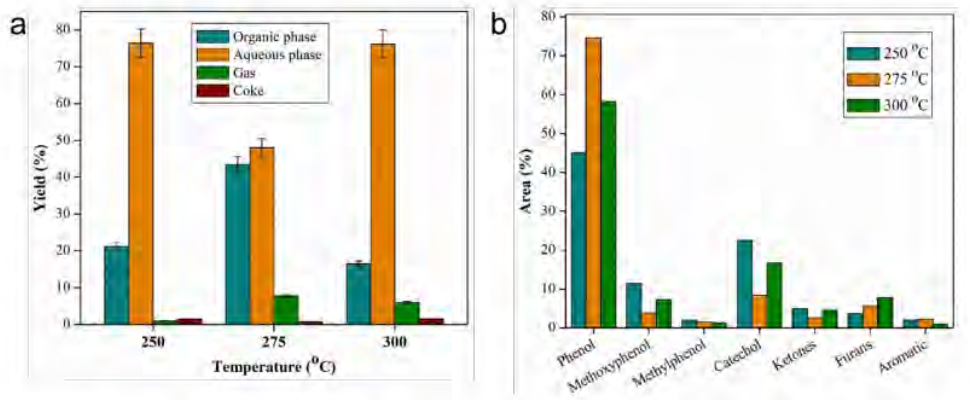

Figure 11. (a) Product distribution of upgraded bio-oil and (b) selectivity of organic phase bio-oil components with ZnO/H-Z catalyst at temperatures of 250, 275, and 300 °C (catalyst loadig of 2.5 wt%, reaction time of 2 hours)

Based on the selectivity data of the bio-oil components in **Figure 11b**, there are significant differences in several groups of compounds observed. The increase in temperature causes an increase in phenol levels, especially when the temperature is 275 °C, with the percentage of phenol area reaching 87%. At this temperature, it is assumed that the highest conversion rate is to convert methoxyphenol into phenol and reduce catechol as an intermediate compound. This is also supported by the percentage area of methoxyphenol and catechol, which is much lower than other temperatures. Temperature is reported to play an active role in the HDO reaction's selectivity by affecting the intermediate's stability. At higher temperatures, the hydrogenation activity decreases due to the reduction in hydrogen adsorption, which is an exothermic reaction. Therefore at high temperatures, more deoxygenation pathways occur compared to hydrogenation [70].

3.8 Effect of catalyst loading

The catalytic activity of a zeolite is closely related to the presence of an active site in the zeolite. Many acid sites increase the possibility of converting oxygenate compounds [71]. Therefore, this study observes the effect of increasing the catalyst mass used during the HDO process. The distribution of the resulting products is summarized in **Figure 12a**, while the selectivity of the upgraded bio-oil content is shown in **Figure 12b**.

Bio-oil catalyzed by a 5.0 wt% catalyst produces more organic phase, gas, and a less aqueous phase than other catalysts. On the other hand, the 7.5 wt% catalysts produce the highest aqueous phase yield but the minor organic phase and gas. This result is in line with that reported by Benés et al. [72], the highest yield of the organic phase is obtained from HDO with a catalyst loading ratio of 5.0 wt%. Up to a catalyst loading ratio of 5%, the removal of oxygen in the form of CO_2 increases significantly. The yield difference produce in this case is related to the number of catalysts used to add to the active sites that play a role during the HDO reaction [73,74]. This can be seen in the 5.0 wt% catalyst, where the amount of gas produced indicates a decarboxylation reaction pathway that produces gases such as CO_2 as one of the by-products of HDO. The amount of water produced in the aqueous phase suggests that the dominant reaction pathway is deoxygenation. On the other hand, an increase in the amount of catalyst above 5.0 wt% indicates an increase in the coke formed. The strong acidity of the support material supports polymerization and condensation reactions that lead to coke formation [75].

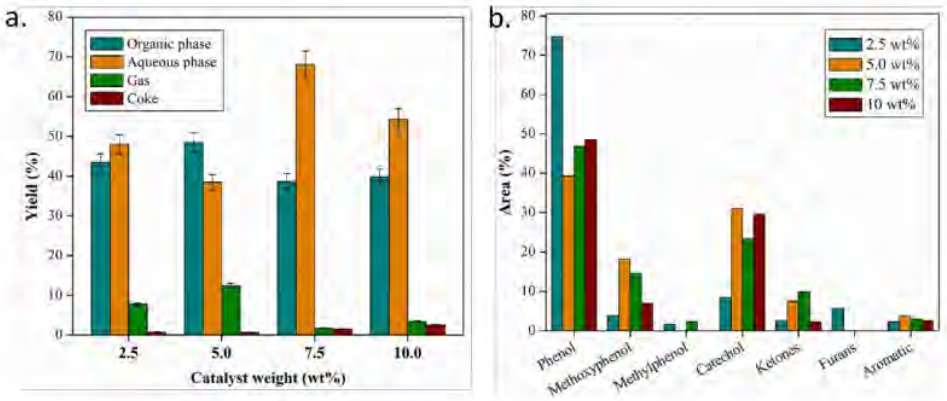

Figure 12. (a) Distribution of upgraded bio-oil product and (b) selectivity of organic phase components catalyzed by ZnO/H-Z with various catalyst masses 2.5, 5.0, 7.5, and 10 wt% (at 275°C for 2 hours)

Based on the data on the selectivity of the compounds produced in the organic phase upgraded bio-oil (**Figure 12**), with the addition of the percentage of the metal as the active site of the catalyst, there is a change in the percentage area of the leading compound group of bio-oil. The comparison between the chromatograms of raw bio-oil and the upgraded product is shown in **Figure 13**. Several compounds, such as phenol and furan, show a significant decrease, while methoxyphenol, catechol, ketone, and aromatic hydrocarbons project an increase. The decline in phenol content occurs due to further reactions during the HDO process. Phenol undergoes a deoxygenation reaction so that it releases oxygen and becomes an aromatic hydrocarbon compound. In the conversion of phenol to aromatic hydrocarbons, the oxide catalyst, in its application as a catalyst, goes through approximately three steps, including chemisorption through the oxygen atom at the unsaturated coordinate metal site, donation of protons from the hydroxyl group, and desorption [76,77]. Further, furan is no longer detected in bio-oil, which is upgraded with a catalyst of 5.0, 7.5, and 10 wt%. It is

presumably due to further conversion of furan to produce ketone compounds, so the percentage of ketone area is relatively increased. However, it is different for the 10 wt% catalyst, which shows a decrease in the percentage of ketone area, but the percentage of 9-tetradecenal and 9-octadecenal areas increase significantly. This is presumably due to ring opening in furans, ketones, and other aromatic compounds to form esters and long chain aldehydes [54].

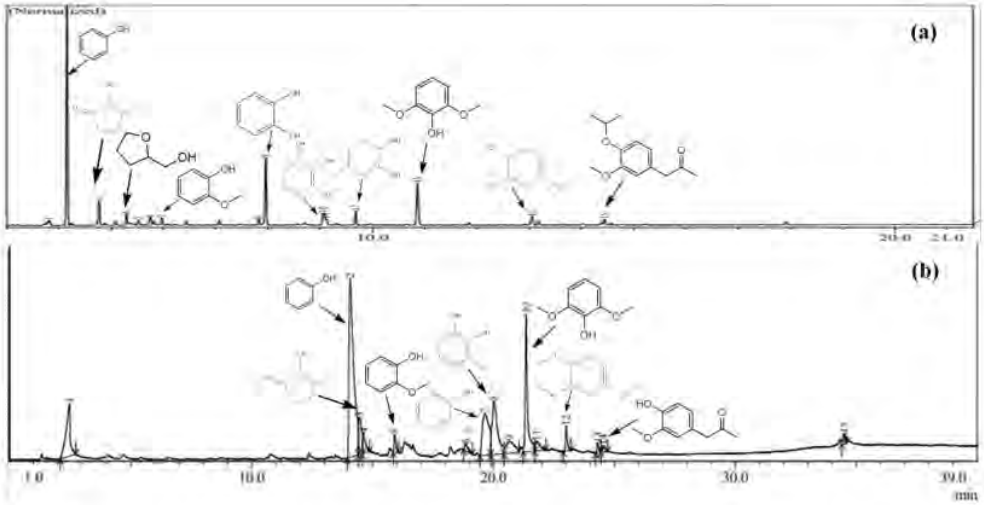

Figure 13. GC-MS chromatograms of (a) raw bio-oil and (b) upgraded product catalyzed by 5 wt% ZnO/HZ at 275 °C.

4. Conclusion

We have presented the performance of natural zeolite (HZ) supported transition metal oxide (TMO) in the bio-oil hydrodeoxygenation process. The Fe_2O_3/HZ, ZnO/HZ, and CuO/HZ catalysts show suitable catalyst characteristics with good crystallinity, large surface area and pore volume, and small pore size that determine catalyst performance (high conversion and selectivity). The optimum temperature is found at 275 °C with ZnO/HZ catalyst 5% wt. with high conversion (~ 50%) for the hydrodeoxygenation process. All refined bio-oil show upgraded physicochemical content, which further proves the

performance of HZ-based TMO catalysts. Therefore, this finding is a step forward to producing a future affordable catalyst by utilizing natural zeolite as a supported catalyst in bio-oil refining through hydrodeoxygenation.

CRediT authorship contribution statement

Junifa Layla Sihombing: Conceptualization, Methodology, Data curation, Writing- original draft, Supervision. **Herlinawati**: Formal analysis, Writing- original draft, Supervision. **Ahmad Nasir Pulungan**: Conceptualization, Supervision, Visualization, Writing- original draft. **Lisnawaty Simatupang**: Methodology, Data curation, Writing- review & editing. **Rahayu**: Investigation, Software, Writing- review & editing. **Ary Anggara Wibowo**: Software, Writing- review & editing.

Declaration of Competing Interest

The authors declare that there is no conflict of interest.

Acknowledgment

The author would like to acknowledge the Rector of Universitas Negeri Medan for the financial support from the 2022 applied product research scheme (No. 104/UN33.8/KEP/PPKM/PT/2022).

References

(1) IEA. Renewables 2021. *International Energy Agency (IEA) Publications International*. **2021**, 167.

(2) Elkasabi, Y.; Mullen, C. A.; Pighinelli, A. L. M. T.; Boateng, A. A. Hydrodeoxygenation of Fast-Pyrolysis Bio-Oils from Various Feedstocks Using Carbon-Supported Catalysts. *Fuel Processing Technology* **2014**, *123*, 11–18. https://doi.org/10.1016/j.fuproc.2014.01.039.

(3) Ahmadi, S.; Yuan, Z.; Rohani, S.; Xu, C. Effects of Nano-Structured CoMo Catalysts on Hydrodeoxygenation of Fast Pyrolysis Oil in Supercritical Ethanol. *Catalysis Today* **2016**, *269*, 182–194. https://doi.org/10.1016/j.cattod.2015.08.040.

(4) Hita, I.; Cordero-Lanzac, T.; Kekälaïnen, T.; Okafor, O.; Rodríguez-Mirasol, J.; Cordero, T.; Bilbao, J.; Jänis, J.; Castano, P. In-Depth Analysis of Raw Bio-Oil and Its Hydrodeoxygenated Products for a Comprehensive Catalyst Performance Evaluation. *ACS Sustainable Chemistry and Engineering* **2020**, *8* (50), 18433–18445. https://doi.org/10.1021/acssuschemeng.0c05533.

(5) Ly, H. V.; Kim, J.; Hwang, H. T.; Choi, J. H.; Woo, H. C.; Kim, S. S. Catalytic Hydrodeoxygenation of Fast Pyrolysis Bio-Oil from Saccharina Japonica Alga for Bio-Oil Upgrading. *Catalysts* **2019**, *9* (12). https://doi.org/10.3390/catal9121043.

(6) Kar, Y. Catalytic Cracking of Pyrolytic Oil by Using Bentonite Clay for Green Liquid Hydrocarbon Fuels Production. *Biomass and Bioenergy* **2018**, *119* (October), 473–479. https://doi.org/10.1016/j.biombioe.2018.10.014.

(7) Chen, G.; Zhang, R.; Ma, W.; Liu, B.; Li, X.; Yan, B.; Cheng, Z.; Wang, T. Catalytic Cracking of Model Compounds of Bio-Oil over HZSM-5 and the Catalyst Deactivation. *Science of the Total Environment* **2018**, *631–632*, 1611–1622. https://doi.org/10.1016/j.scitotenv.2018.03.147.

(8) Li, S.; Zhang, S.; Feng, Z.; Yan, Y. Coke Formation in the Catalytic Cracking of Bio-Oil Model Compounds. *Environmental Progress & Sustainable Energy* **2015**, *34* (1), 240–247. https://doi.org/https://doi.org/10.1002/ep.11936.

(9) Zhang, H.; Yang, C.; Tao, Y.; Chen, M.; Xiao, R. Catalytic Cracking of Model Compounds of Bio-Oil: Characteristics and Mechanism Research on Guaiacol and Acetic Acid. *Fuel Processing Technology* **2022**, *238*, 107512. https://doi.org/https://doi.org/10.1016/j.fuproc.2022.107512.

(10) Mortensen, P. M.; Grunwaldt, J. D.; Jensen, P. A.; Jensen, A. D. Screening of Catalysts for Hydrodeoxygenation of Phenol as a Model Compound for Bio-Oil. *ACS Catalysis* **2013**, *3* (8), 1774–1785. https://doi.org/10.1021/cs400266e.

(11) Benés, M.; Bilbao, R.; Santos, J. M.; Alves Melo, J.; Wisniewski, A.; Fonts, I. Hydrodeoxygenation of Lignocellulosic Fast Pyrolysis Bio-Oil: Characterization of the Products and Effect of the Catalyst Loading Ratio. *Energy and Fuels* **2019**, *33* (5), 4272–4286. https://doi.org/10.1021/acs.energyfuels.9b00265.

(12) Roldugina, E. A.; Naranov, E. R.; Maximov, A. L.; Karakhanov, E. A. Hydrodeoxygenation of Guaiacol as a Model Compound of Bio-Oil in Methanol over Mesoporous Noble Metal Catalysts. *Applied Catalysis A: General* **2018**, *553*, 24–35. https://doi.org/10.1016/j.apcata.2018.01.008.

(13) Cordero-Lanzac, T.; Rodríguez-Mirasol, J.; Cordero, T.; Bilbao, J. Advances and Challenges in the Valorization of Bio-Oil: Hydrodeoxygenation Using Carbon-Supported Catalysts. *Energy and Fuels* **2021**, *35* (21), 17008–17031. https://doi.org/10.1021/acs.energyfuels.1c01700.

(14) Alvarez-Galvan, M. C.; Campos-Martin, J. M.; Fierro, J. L. G. Transition Metal Phosphides for the Catalytic Hydrodeoxygenation of Waste Oils into Green Diesel. *Catalysts* **2019**, *9* (3). https://doi.org/10.3390/catal9030293.

(15) Gea, S.; Hutapea, Y. A.; Piliang, A. F. R.; Pulungan, A. N.; Rahayu, R.; Layla, J.; Tikoalu, A. D.; Wijaya, K.; Saputri, W. D. A Comprehensive Review of Experimental Parameters in Bio-Oil Upgrading from Pyrolysis of Biomass to Biofuel Through Catalytic Hydrodeoxygenation. *Bioenergy Research* **2022**. https://doi.org/10.1007/s12155-022-10438-w.

(16) Wang, X.; Arai, M.; Wu, Q.; Zhang, C.; Zhao, F. Hydrodeoxygenation of Lignin-Derived Phenolics-a Review on the Active Sites of Supported Metal Catalysts. *Green Chemistry* **2020**, *22* (23), 8140–8168. https://doi.org/10.1039/d0gc02610g.

(17) Li, X.; Chen, G.; Liu, C.; Ma, W.; Yan, B.; Zhang, J. Hydrodeoxygenation of Lignin-Derived Bio-Oil Using Molecular Sieves Supported Metal Catalysts : A Critical Review. *Renewable and Sustainable Energy Reviews* **2016**, No. December, 0–1. https://doi.org/10.1016/j.rser.2016.12.057.

(18) Wang, Y.; Wu, J.; Wang, S. Hydrodeoxygenation of Bio-Oil over Pt-Based Supported Catalysts: Importance of Mesopores and Acidity of the Support to Compounds with Different Oxygen Contents. *RSC Advances* **2013**, *3* (31), 12635–12640. https://doi.org/10.1039/c3ra41405a.

(19) Gea, S.; Irvan; Wijaya, K.; Nadia, A.; Pulungan, A. N.; Sihombing, J. L.; Rahayu. Bio-Oil Hydrodeoxygenation over Zeolite-Based Catalyst: The Effect of Zeolite Activation and Nickel Loading on Product Characteristics. *International Journal of Energy and Environmental Engineering* **2022**, *13* (2), 541–553. https://doi.org/10.1007/s40095-021-00467-0.

(20) Gea, S.; Irvan, I.; Wijaya, K.; Nadia, A.; Pulungan, A. N.; Sihombing, J. L.; Rahayu, R. Bio-Oil Hydrodeoxygenation over Acid Activated-Zeolite with Different Si/Al Ratio. *Biofuel Research Journal* **2022**, *9* (2), 1630–1639. https://doi.org/10.18331/brj2022.9.2.4.

(21) Sihombing, J. L.; Gea, S.; Wirjosentono, B.; Agusnar, H.; Pulungan, A. N.; Herlinawati, H.; Yusuf, M. Characteristic and Catalytic Performance of Co and Co-Mo Metal Impregnated in Sarulla Natural Zeolite Catalyst for Hydrocracking of MEFA Rubber Seed Oil into Biogasoline Fraction. *Catalysts* **2020**, *10*, 121.

(22) Oh, S.; Hwang, H.; Choi, H. S.; Choi, J. W. The Effects of Noble Metal Catalysts on the Bio-Oil Quality during the Hydrodeoxygenative Upgrading Process. *Fuel* **2015**, *153*, 535–543. https://doi.org/10.1016/j.fuel.2015.03.030.

(23) Sheng, C.; Azevedo, J. L. T. Estimating the Higher Heating Value of Biomass Fuels from Basic Analysis Data. *Biomass and Bioenergy* **2005**, *28* (5), 499–507. https://doi.org/10.1016/j.biombioe.2004.11.008.

(24) Khawas, P.; Deka, S. C. Isolation and Characterization of Cellulose Nanofibers from Culinary Banana Peel Using High-Intensity Ultrasonication Combined with Chemical Treatment. *Carbohydrate Polymers* **2016**, *137*, 608–616. https://doi.org/https://doi.org/10.1016/j.carbpol.2015.11.020.

(25) Sriningsih, W.; Saerodji, M. G.; Trisunaryanti, W.; Triyono; Armunanto, R.; Falah, I. I. Fuel Production from LDPE Plastic Waste over Natural Zeolite Supported Ni, Ni-Mo, Co and Co-Mo Metals. *Procedia Environmental Sciences* **2014**, *20*, 215–224. https://doi.org/10.1016/j.proenv.2014.03.028.

(26) Hao, J.; Qi, B.; Li, D.; Zeng, F. Catalytic Co-Pyrolysis of Rice Straw and Ulva Prolifera Macroalgae: Effects of Process Parameter on Bio-Oil up-Gradation. *Renewable Energy* **2021**, *164*, 460–471. https://doi.org/10.1016/j.renene.2020.09.056.

(27) Miao, C.; Zhou, G.; Chen, S.; Xie, H.; Zhang, X. Synergistic Effects between Cu and Ni Species in NiCu/γ-Al2O3 Catalysts for Hydrodeoxygenation of Methyl Laurate. *Renewable Energy* **2020**, *153*, 1439–1454. https://doi.org/10.1016/j.renene.2020.02.099.

(28) Pulungan, A. N.; Kembaren, A.; Nurfajriani, N.; Syuhada, F. A.; Sihombing, J. L.; Yusuf, M.; Rahayu, R. Biodiesel Production from Rubber Seed Oil Using Natural Zeolite Supported Metal Oxide Catalysts. *Polish Journal of Environmental Studies* **2021**, *30* (6), 5681–5689. https://doi.org/10.15244/pjoes/135615.

(29) Shwan, S.; Jansson, J.; Olsson, L.; Skoglundh, M. Chemical Deactivation of Fe-BEA as NH3-SCR Catalyst-Effect of Phosphorous. *Applied Catalysis B: Environmental* **2014**, *147*, 111–123. https://doi.org/10.1016/j.apcatb.2013.08.042.

(30) Pulungan, A. N.; Kembaren, A.; Nurfajriani, N.; Syuhada, F. A.; Sihombing, J. L.; Yusuf, M.; Rahayu, R. Biodiesel Production from Rubber Seed Oil Using Natural Zeolite Supported Metal Oxide Catalysts. *Polish Journal of Environmental Studies* **2021**, *30* (6), 5681–5689. https://doi.org/10.15244/pjoes/135615.

(31) Chu, R.; Yang, D.; Meng, X.; Yu, S.; Wan, Y.; Wu, J.; Wang, J. Effect of Surface Structure and Adsorption Activity on Implanting of B-Oriented ZSM-5 Zeolite Film on Modified α-Quartz Substrate. *Frontiers in Chemistry* **2019**, *7* (September), 1–12. https://doi.org/10.3389/fchem.2019.00636.

(32) Han, J.; Liu, D. Influence of Synthesis Conditions on the Mesopore Distribution and Morphology Control of Hierarchical ZSM-5 Zeolites Synthesized by Double-Acyloxy

Organosilane Surfactants. *European Journal of Inorganic Chemistry* **2015**, *2015* (30), 5081–5088. https://doi.org/10.1002/ejic.201500735.

(33) Sihombing, J. L.; Gea, S.; Wirjosentono, B.; Agusnar, H.; Pulungan, A. N.; Herlinawati, H.; Yusuf, M. Characteristic and Catalytic Performance of Co and Co-Mo Metal Impregnated in Sarulla Natural Zeolite Catalyst for Hydrocracking of MEFA Rubber Seed Oil into Biogasoline Fraction. *Catalysts* **2020**, *10*, 121.

(34) Kurnia, I.; Karnjanakom, S.; Bayu, A.; Yoshida, A.; Rizkiana, J.; Prakoso, T.; Abudula, A.; Guan, G. In-Situ Catalytic Upgrading of Bio-Oil Derived from Fast Pyrolysis of Lignin over High Aluminum Zeolites. *Fuel Processing Technology* **2017**, *167* (August), 730–737. https://doi.org/10.1016/j.fuproc.2017.08.026.

(35) Widayatno, W. B.; Guan, G.; Rizkiana, J.; Yang, J.; Hao, X.; Tsutsumi, A.; Abudula, A. Upgrading of Bio-Oil from Biomass Pyrolysis over Cu-Modified β-Zeolite Catalyst with High Selectivity and Stability. *Applied Catalysis B: Environmental* **2016**, *186*, 166–172. https://doi.org/10.1016/j.apcatb.2016.01.006.

(36) Elkasabi, Y.; Mullen, C. A.; Pighinelli, A. L. M. T.; Boateng, A. A. Hydrodeoxygenation of Fast-Pyrolysis Bio-Oils from Various Feedstocks Using Carbon-Supported Catalysts. *Fuel Processing Technology* **2014**, *123*, 11–18. https://doi.org/10.1016/j.fuproc.2014.01.039.

(37) Huang, Z.; Qin, L.; Xu, Z.; Chen, W.; Xing, F.; Han, J. The Effects of Fe2O3 Catalyst on the Conversion of Organic Matter and Bio-Fuel Production during Pyrolysis of Sewage Sludge. *Journal of the Energy Institute* **2019**, *92* (4), 835–842. https://doi.org/10.1016/j.joei.2018.06.015.

(38) Konadu, D.; Kwawu, C. R.; Tia, R.; Adei, E.; de Leeuw, N. H. Mechanism of Guaiacol Hydrodeoxygenation on Cu (111): Insights from Density Functional Theory Studies. *Catalysts* 2021, 11 (4), 523. https://doi.org/10.3390/catal11040523.

(39) Leal, F.; Teixeira, V.; Edral, M.; Souza, F. Bio-Oil Hydrotreating Using Nickel Phosphides Supported on Carbon-Covered Alumina. *Fuel* **2019**, *241* (October 2018), 686–694. https://doi.org/10.1016/j.fuel.2018.12.063.

(40) Kim, T. S.; Oh, S.; Kim, J. Y.; Choi, I. G.; Choi, J. W. Study on the Hydrodeoxygenative Upgrading of Crude Bio-Oil Produced from Woody Biomass by Fast Pyrolysis. *Energy* **2014**, *68*, 437–443. https://doi.org/10.1016/j.energy.2014.03.004.

(41) Baloch, H. A.; Nizamuddin, S.; Siddiqui, M. T. H.; Riaz, S.; Konstas, K.; Mubarak, N. M.; Srinivasan, M. P.; Griffin, G. J. Catalytic Upgradation of Bio-Oil over Metal Supported Activated Carbon Catalysts in Sub-Supercritical Ethanol. *Journal of Environmental Chemical Engineering* **2021**, *9* (2), 105059. https://doi.org/10.1016/j.jece.2021.105059.

(42) Oh, S.; Lee, J. H.; Choi, I. G.; Choi, J. W. Enhancement of Bio-Oil Hydrodeoxygenation Activity over Ni-Based Bimetallic Catalysts Supported on SBA-15. *Renewable Energy* **2020**, *149*, 1–10. https://doi.org/10.1016/j.renene.2019.12.027.

(43) Kurnia, I.; Karnjanakom, S.; Bayu, A.; Yoshida, A.; Rizkiana, J.; Prakoso, T.; Abudula, A.; Guan, G. In-Situ Catalytic Upgrading of Bio-Oil Derived from Fast Pyrolysis of Lignin over High Aluminum Zeolites. *Fuel Processing Technology* **2017**, *167* (August), 730–737. https://doi.org/10.1016/j.fuproc.2017.08.026.

(44) Parsell, T. H.; Owen, B. C.; Klein, I.; Jarrell, T. M.; Marcum, C. L.; Haupert, L. J.; Amundson, L. M.; Kenttämaa, H. I.; Ribeiro, F.; Miller, J. T.; Abu-Omar, M. M.

Cleavage and Hydrodeoxygenation (HDO) of C-O Bonds Relevant to Lignin Conversion Using Pd/Zn Synergistic Catalysis. *Chemical Science* **2013**, *4* (2), 806–813. https://doi.org/10.1039/c2sc21657d.

(45) Spanjers, C. S.; Sim, R. S.; Sturgis, N. P.; Kabius, B.; Rioux, R. M. In Situ Spectroscopic Characterization of Ni1- XZnx/ZnO Catalysts and Their Selectivity for Acetylene Semihydrogenation in Excess Ethylene. *ACS Catalysis* **2015**, *5* (6), 3304–3315. https://doi.org/10.1021/acscatal.5b00627.

(46) Oh, S.; Lee, J. H.; Choi, I. G.; Choi, J. W. Enhancement of Bio-Oil Hydrodeoxygenation Activity over Ni-Based Bimetallic Catalysts Supported on SBA-15. *Renewable Energy* **2020**, *149*, 1–10. https://doi.org/10.1016/j.renene.2019.12.027.

(47) Grioui, N.; Halouani, K.; Agblevor, F. A. Bio-Oil from Pyrolysis of Tunisian Almond Shell: Comparative Study and Investigation of Aging Effect during Long Storage. *Energy for Sustainable Development* **2014**, *21* (1), 100–112. https://doi.org/10.1016/j.esd.2014.05.006.

(48) Dwiatmoko, A. A.; Lee, S.; Ham, H. C.; Choi, J. W.; Suh, D. J.; Ha, J. M. Effects of Carbohydrates on the Hydrodeoxygenation of Lignin-Derived Phenolic Compounds. *ACS Catalysis* **2015**, *5* (1), 433–437. https://doi.org/10.1021/cs501567x.

(49) Leal, F.; Teixeira, V.; Edral, M.; Souza, F. Bio-Oil Hydrotreating Using Nickel Phosphides Supported on Carbon-Covered Alumina. *Fuel* **2019**, *241* (October 2018), 686–694. https://doi.org/10.1016/j.fuel.2018.12.063.

(50) Oh, S.; Hwang, H.; Choi, H. S.; Choi, J. W. The Effects of Noble Metal Catalysts on the Bio-Oil Quality during the Hydrodeoxygenative Upgrading Process. *Fuel* **2015**, *153*, 535–543. https://doi.org/10.1016/j.fuel.2015.03.030.

(51) Gea, S.; Haryono, A.; Andriayani, A.; Sihombing, J. L. The Stabilization of Liquid Smoke through Hydrodeoxygenation Over Nickel Catalyst Loaded on Sarulla Natural Zeolite. *Applied Sciences* **2020**, *10*, 1–17.

(52) Liu, L. J.; Liu, Y. G.; Gao, X.; Zhang, R. Q.; Zhai, Y. P. Hydrodeoxygenation of Bio-Oil Model Compounds over Amorphous NiB/SiO2-Al2O3 Catalyst in Oil-Water Biphasic System. *Ranliao Huaxue Xuebao/Journal of Fuel Chemistry and Technology* **2017**, *45* (8), 932–938. https://doi.org/10.1016/s1872-5813(17)30044-0.

(53) Venkatesan, K.; Krishna, J. V. J.; Anjana, S.; Selvam, P.; Vinu, R. Hydrodeoxygenation Kinetics of Syringol, Guaiacol and Phenol over H-ZSM-5. *Catalysis Communications* **2021**, *148*. https://doi.org/10.1016/j.catcom.2020.106164.

(54) Oh, S.; Hwang, H.; Choi, H. S.; Choi, J. W. The Effects of Noble Metal Catalysts on the Bio-Oil Quality during the Hydrodeoxygenative Upgrading Process. *Fuel* **2015**, *153*, 535–543. https://doi.org/10.1016/j.fuel.2015.03.030.

(55) Shafaghat, H.; Rezaei, P. S.; Ashri Wan Daud, W. M. Effective Parameters on Selective Catalytic Hydrodeoxygenation of Phenolic Compounds of Pyrolysis Bio-Oil to High-Value Hydrocarbons. *RSC Advances* **2015**, *5* (126), 103999–104042. https://doi.org/10.1039/c5ra22137d.

(56) Teixeira Cardoso, A. R.; Conrado, N. M.; Krause, M. C.; Bjerk, T. R.; Krause, L. C.; Caramão, E. B. Chemical Characterization of the Bio-Oil Obtained by Catalytic Pyrolysis of Sugarcane Bagasse (Industrial Waste) from the Species Erianthus Arundinaceus. *Journal of Environmental Chemical Engineering* **2019**, *7* (2), 102970. https://doi.org/10.1016/j.jece.2019.102970.

(57) He, Z.; Wang, X. Hydrodeoxygenation of Model Compounds and Catalytic Systems for Pyrolysis Bio-Oils Upgrading. *Catalysis for Sustainable Energy* **2013**, *1*, 28–52. https://doi.org/10.2478/cse-2012-0004.

(58) Botas, J. A.; Serrano, D. P.; García, A.; Ramos, R. Catalytic Conversion of Rapeseed Oil for the Production of Raw Chemicals, Fuels and Carbon Nanotubes over Ni-Modified Nanocrystalline and Hierarchical ZSM-5. *Applied Catalysis B: Environmental* **2014**, *145*, 205–215. https://doi.org/10.1016/j.apcatb.2012.12.023.

(59) Olcese, R. N.; Bettahar, M.; Petitjean, D.; Malaman, B.; Giovanella, F.; Dufour, A. Gas-Phase Hydrodeoxygenation of Guaiacol over Fe/SiO 2 Catalyst. *Applied Catalysis B: Environmental* **2012**, *115–116*, 63–73. https://doi.org/10.1016/j.apcatb.2011.12.005.

(60) Shafaghat, H.; Rezaei, P. S.; Daud, W. M. A. W. Catalytic Hydrodeoxygenation of Simulated Phenolic Bio-Oil to Cycloalkanes and Aromatic Hydrocarbons over Bifunctional Metal/Acid Catalysts of Ni/HBeta, Fe/HBeta and NiFe/HBeta. *Journal of Industrial and Engineering Chemistry* **2016**, *35*, 268–276. https://doi.org/10.1016/j.jiec.2016.01.001.

(61) Awan, I. Z.; Beltrami, G.; Bonincontro, D.; Gimello, O.; Cacciaguerra, T.; Tanchoux, N.; Martucci, A.; Albonetti, S.; Cavani, F.; Di Renzo, F. Copper-Nickel Mixed Oxide Catalysts from Layered Double Hydroxides for the Hydrogen-Transfer Valorisation of Lignin in Organosolv Pulping. *Applied Catalysis A: General* **2021**, *609*. https://doi.org/10.1016/j.apcata.2020.117929.

(62) Gabrysch, T.; Peng, B.; Bunea, S.; Dyker, G.; Muhler, M. The Role of Metallic Copper in the Selective Hydrodeoxygenation of Glycerol to 1,2-Propanediol over Cu/ZrO2. *ChemCatChem* **2018**, *10* (6), 1344–1350. https://doi.org/10.1002/cctc.201701748.

(63) Wang, Q.; Yu, Z.; Feng, J.; Fornasiero, P.; He, Y.; Li, D. Insight into the Effect of Dual Active Cu/Cu+Sites in a Cu/ZnO-Al2O3Catalyst on 5-Hydroxylmethylfurfural Hydrodeoxygenation. *ACS Sustainable Chemistry and Engineering* **2020**, *8* (40), 15288–15298. https://doi.org/10.1021/acssuschemeng.0c05235.

(64) He, Z.; Wang, X. Hydrodeoxygenation of Model Compounds and Catalytic Systems for Pyrolysis Bio-Oils Upgrading. *Catalysis for Sustainable Energy* **2013**, *1*, 28–52. https://doi.org/10.2478/cse-2012-0004.

(65) Moberg, D. R.; Thibodeau, T. J.; Amar, F. G.; Frederick, B. G. Mechanism of Hydrodeoxygenation of Acrolein on a Cluster Model of MoO 3. *Journal of Physical Chemistry C* **2010**, *114* (32), 13782–13795. https://doi.org/10.1021/jp104421a.

(66) Pourzolfaghar, H.; Abnisa, F.; Wan Daud, W. M. A.; Aroua, M. K. Atmospheric Hydrodeoxygenation of Bio-Oil Oxygenated Model Compounds: A Review. *Journal of Analytical and Applied Pyrolysis* **2018**, *133*, 117–127. https://doi.org/10.1016/j.jaap.2018.04.013.

(67) Ahmadi, S.; Reyhanitash, E.; Yuan, Z.; Rohani, S.; Xu, C. (Charles). Upgrading of Fast Pyrolysis Oil via Catalytic Hydrodeoxygenation: Effects of Type of Solvents. *Renewable Energy* **2017**, *114*, 376–382. https://doi.org/10.1016/j.renene.2017.07.041.

(68) Cheng, S.; Wei, L.; Julson, J.; Muthukumarappan, K.; Kharel, P. R.; Cao, Y.; Boakye, E.; Raynie, D.; Gu, Z. Hydrodeoxygenation Upgrading of Pine Sawdust Bio-Oil Using Zinc Metal with Zero Valency. *Journal of the Taiwan Institute of Chemical Engineers* **2017**, *74*, 146–153. https://doi.org/10.1016/j.jtice.2017.02.011.

(69) Kim, T. S.; Oh, S.; Kim, J. Y.; Choi, I. G.; Choi, J. W. Study on the Hydrodeoxygenative Upgrading of Crude Bio-Oil Produced from Woody Biomass by

Fast Pyrolysis. *Energy* **2014**, *68*, 437–443. https://doi.org/10.1016/j.energy.2014.03.004.

(70) Shafaghat, H.; Rezaei, P. S.; Ashri Wan Daud, W. M. Effective Parameters on Selective Catalytic Hydrodeoxygenation of Phenolic Compounds of Pyrolysis Bio-Oil to High-Value Hydrocarbons. *RSC Advances* **2015**, *5* (126), 103999–104042. https://doi.org/10.1039/c5ra22137d.

(71) Lee, H.; Kim, H.; Yu, M. J.; Ko, C. H.; Jeon, J. K.; Jae, J.; Park, S. H.; Jung, S. C.; Park, Y. K. Catalytic Hydrodeoxygenation of Bio-Oil Model Compounds over Pt/HY Catalyst. *Scientific Reports* **2016**, *6*, 1–8. https://doi.org/10.1038/srep28765.

(72) Benés, M.; Bilbao, R.; Santos, J. M.; Alves Melo, J.; Wisniewski, A.; Fonts, I. Hydrodeoxygenation of Lignocellulosic Fast Pyrolysis Bio-Oil: Characterization of the Products and Effect of the Catalyst Loading Ratio. *Energy and Fuels* **2019**, *33* (5), 4272–4286. https://doi.org/10.1021/acs.energyfuels.9b00265.

(73) Sankaranarayanan, T. M.; Berenguer, A.; Ochoa-Hernández, C.; Moreno, I.; Jana, P.; Coronado, J. M.; Serrano, D. P.; Pizarro, P. Hydrodeoxygenation of Anisole as Bio-Oil Model Compound over Supported Ni and Co Catalysts: Effect of Metal and Support Properties. *Catalysis Today* **2015**, *243* (C), 163–172. https://doi.org/10.1016/j.cattod.2014.09.004.

(74) Roldugina, E. A.; Naranov, E. R.; Maximov, A. L.; Karakhanov, E. A. Hydrodeoxygenation of Guaiacol as a Model Compound of Bio-Oil in Methanol over Mesoporous Noble Metal Catalysts. *Applied Catalysis A: General* **2018**, *553*, 24–35. https://doi.org/10.1016/j.apcata.2018.01.008.

(75) Nava, R.; Pawelec, B.; Castaño, P.; Álvarez-Galván, M. C.; Loricera, C. V.; Fierro, J. L. G. Upgrading of Bio-Liquids on Different Mesoporous Silica-Supported CoMo

Catalysts. *Applied Catalysis B: Environmental* **2009**, *92* (1–2), 154–167. https://doi.org/10.1016/j.apcatb.2009.07.014.

(76) Moberg, D. R.; Thibodeau, T. J.; Amar, F. G.; Frederick, B. G. Mechanism of Hydrodeoxygenation of Acrolein on a Cluster Model of MoO 3. *Journal of Physical Chemistry C* **2010**, *114* (32), 13782–13795. https://doi.org/10.1021/jp104421a.

(77) Mortensen, P. M.; Grunwaldt, J. D.; Jensen, P. A.; Jensen, A. D. Screening of Catalysts for Hydrodeoxygenation of Phenol as a Model Compound for Bio-Oil. *ACS Catalysis* **2013**, *3* (8), 1774–1785. https://doi.org/10.1021/cs400266e.

Dr. Junifa Layla Sihombing, M.Sc_4

ORIGINALITY REPORT

28%	17%	24%	4%
SIMILARITY INDEX	INTERNET SOURCES	PUBLICATIONS	STUDENT PAPERS

PRIMARY SOURCES

1	digilib.unimed.ac.id Internet Source	4%
2	link.springer.com Internet Source	3%
3	www.mdpi.com Internet Source	2%
4	Mario Benés, Rafael Bilbao, Jandyson Machado Santos, Josué Alves Melo, Alberto Wisniewski, Isabel Fonts. "Hydrodeoxygenation of Lignocellulosic Fast Pyrolysis Bio-Oil: Characterization of the Products and Effect of the Catalyst Loading Ratio", Energy & Fuels, 2019 Publication	1%
5	Lujiang Xu, Qian Yao, Ying Zhang, Yao Fu. " Integrated Production of Aromatic Amines and N-Doped Carbon from Lignin via Catalytic Fast Pyrolysis in the Presence of Ammonia over Zeolites ", ACS Sustainable Chemistry & Engineering, 2017 Publication	1%

6	s-space.snu.ac.kr Internet Source	1 %
7	Adistya Husna, Fitria Febrianti, Habibie Syah, Rabiatul Pangaribuan, Tia Surbakti, Junifa Sihombing, Ahmad Pulungan. "Conversion of Cellulose From Palm Oil Middle Waste (Elaeis Guineensis) Into Bio-Oil Products As Alternative Fuel", Egyptian Journal of Chemistry, 2022 Publication	1 %
8	www.biofueljournal.com Internet Source	1 %
9	www.researchgate.net Internet Source	1 %
10	Wahyu Bambang Widayatno, Guoqing Guan, Jenny Rizkiana, Jingxuan Yang, Xiaogang Hao, Atsushi Tsutsumi, Abuliti Abudula. "Upgrading of bio-oil from biomass pyrolysis over Cu-modified β-zeolite catalyst with high selectivity and stability", Applied Catalysis B: Environmental, 2016 Publication	1 %
11	He, Zhong, and Xianqin Wang. "Renewable energy and fuel production over transition metal oxides: The role of oxygen defects and acidity", Catalysis Today, 2015. Publication	<1 %

12	Zhong He, Xianqin Wang. "Hydrodeoxygenation of model compounds and catalytic systems for pyrolysis bio-oils upgrading", Catalysis for Sustainable Energy, 2012 Publication	<1 %
13	Submitted to Leeds Beckett University Student Paper	<1 %
14	"Sustainable Energy Technology and Policies", Springer Nature, 2018 Publication	<1 %
15	Hoda Shafaghat, Pouya Sirous Rezaei, Wan Mohd Ashri Wan Daud. "Effective parameters on selective catalytic hydrodeoxygenation of phenolic compounds of pyrolysis bio-oil to high-value hydrocarbons", RSC Advances, 2015 Publication	<1 %
16	Xiangping Li, Guanyi Chen, Caixia Liu, Wenchao Ma, Beibei Yan, Jianguang Zhang. "Hydrodeoxygenation of lignin-derived bio-oil using molecular sieves supported metal catalysts: A critical review", Renewable and Sustainable Energy Reviews, 2017 Publication	<1 %
17	studentsrepo.um.edu.my Internet Source	<1 %

18	res.mdpi.com Internet Source	<1 %
19	Shouyun Cheng, Lin Wei, James Julson, Kasiviswanathan Muthukumarappan, Parashu Ram Kharel, Eric Boakye. "Hydrocarbon bio-oil production from pyrolysis bio-oil using non-sulfide Ni-Zn/Al 2 O 3 catalyst", Fuel Processing Technology, 2017 Publication	<1 %
20	Submitted to University of Strathclyde Student Paper	<1 %
21	"Chemical Catalysts for Biomass Upgrading", Wiley, 2020 Publication	<1 %
22	Bingbing Qiu, Xuedong Tao, Jiahao Wang, Ya Liu, Sitong Li, Huaqiang Chu. "Research progress in the preparation of high-quality liquid fuels and chemicals by catalytic pyrolysis of biomass: A review", Energy Conversion and Management, 2022 Publication	<1 %
23	acikbilim.yok.gov.tr Internet Source	<1 %
24	jurnal.ar-raniry.ac.id Internet Source	<1 %
25	www.hindawi.com Internet Source	

<1 %

26 xin chao Wang, Masahiko Arai, Qifan Wu, Chao Zhang, Fengyu Zhao. "Hydrodeoxygenation of lignin-derived phenolics - a review on the active sites of supported metal catalysts", Green Chemistry, 2020 <1 %
Publication

27 D. P. Serrano, J. Aguado, J. M. Escola. "Developing Advanced Catalysts for the Conversion of Polyolefinic Waste Plastics into Fuels and Chemicals", ACS Catalysis, 2012 <1 %
Publication

28 Saharman Gea, Irvan, Karna Wijaya, Asma Nadia, Ahmad Nasir Pulungan, Junifa Layla Sihombing, Rahayu. "Bio-oil hydrodeoxygenation over zeolite-based catalyst: the effect of zeolite activation and nickel loading on product characteristics", International Journal of Energy and Environmental Engineering, 2022 <1 %
Publication

29 Shinyoung Oh, Jae Hoon Lee, In-Gyu Choi, Joon Weon Choi. "Enhancement of bio-oil hydrodeoxygenation activity over Ni-based bimetallic catalysts supported on SBA-15", Renewable Energy, 2020 <1 %

Publication

30	Submitted to University of the Highlands and Islands Millennium Institute Student Paper	<1 %
31	Anamaria Paiva Pinheiro Pires, Jesus Arauzo, Isabel Fonts, Marcelo E. Domine et al. "Challenges and Opportunities for Bio-oil Refining: A Review", Energy & Fuels, 2019 Publication	<1 %
32	Submitted to University of Florida Student Paper	<1 %
33	www.frontiersin.org Internet Source	<1 %
34	Marti Hitsmi, Mochamad Lutfi Firdaus, Nurhamidah Nurhamidah. "PENGEMBANGAN METODE CITRA DIGITAL BERBASIS APLIKASI ANDROID UNTUK ANALISIS ION LOGAM Cr(VI)", Alotrop, 2019 Publication	<1 %
35	Rubén Ramos, Alicia García, Juan A. Botas, David P. Serrano. "Enhanced Production of Aromatic Hydrocarbons by Rapeseed Oil Conversion over Ga and Zn Modified ZSM-5 Catalysts", Industrial & Engineering Chemistry Research, 2016 Publication	<1 %
36	Submitted to University of Birmingham	

	Student Paper	<1%
37	academic.hep.com.cn Internet Source	<1%
38	hdl.handle.net Internet Source	<1%
39	Han-Bing Gao, Le-Le Qiu, Fa-Peng Wu, Jian Xiao, Yun-Peng Zhao, Jing Liang, Yong-Hui Bai, Fang-Jing Liu, Jing-Pei Cao. "Highly efficient catalytic hydrogenolysis of lignin model compounds over hydrotalcite-derived Ni/Al2O3 catalysts", Fuel, 2023 Publication	<1%
40	Hong, Yongchun, He Zhang, Junming Sun et al. "Synergistic Catalysis between Pd and Fe in Gas Phase Hydrodeoxygenation of m-Cresol", ACS Catalysis Publication	<1%
41	Ravinder Kumar, Vladimir Strezov, Tao Kan, Haftom Weldekidan, Jing He, Sayka Jahan. " Investigating the Effect of Mono- and Bimetallic/Zeolite Catalysts on Hydrocarbon Production during Bio-oil Upgrading from Pyrolysis of Biomass ", Energy & Fuels, 2019 Publication	<1%
42	Submitted to University of Newcastle Student Paper	<1%

43	Wei Zhang, Jinzhu Chen, Ruliang Liu, Shengpei Wang, Limin Chen, Kegui Li. "Hydrodeoxygenation of Lignin-Derived Phenolic Monomers and Dimers to Alkane Fuels over Bifunctional Zeolite-Supported Metal Catalysts", ACS Sustainable Chemistry & Engineering, 2014 Publication	<1 %
44	Wu-Jun Liu, Wen-Wei Li, Hong Jiang, Han-Qing Yu. "Fates of Chemical Elements in Biomass during Its Pyrolysis", Chemical Reviews, 2017 Publication	<1 %
45	Xun Hu, Zhanming Zhang, Mortaza Gholizadeh, Shu Zhang, Chun Ho Lam, Zhe Xiong, Yi Wang. "Coke Formation during Thermal Treatment of Bio-oil", Energy & Fuels, 2020 Publication	<1 %
46	Zhong He, Xianqin Wang. "Renewable energy and fuel production over transition metal oxides: The role of oxygen defects and acidity", Catalysis Today, 2015 Publication	<1 %
47	hal.archives-ouvertes.fr Internet Source	<1 %
48	pubs.rsc.org Internet Source	<1 %

49	Lijun Zhang, Xun Hu, Chao Li, Shu Zhang, Yi Wang, Vahideh Esmaeili, Mortaza Gholizadeh. "Fates of heavy organics of bio-oil in hydrotreatment: The key challenge in the way from biomass to biofuel", Science of The Total Environment, 2021 Publication	<1 %
50	M. M. Pedroza, J. F. Souza, G. E. G. Vieira, M. B. D. Bezerra. "BIO-OIL AND BIOGAS FROM THE PYROLYSIS OF SEWAGE SLUDGE, AND NON-ISOTHERMAL DEGRADATION ON USY ZEOLITE", Brazilian Journal of Petroleum and Gas, 2017 Publication	<1 %
51	Qian Wang, Zhi Yu, Junting Feng, Paolo Fornasiero, Yufei He, Dianqing Li. " Insight into the Effect of Dual Active Cu /Cu Sites in a Cu/ZnO-Al O Catalyst on 5-Hydroxylmethylfurfural Hydrodeoxygenation ", ACS Sustainable Chemistry & Engineering, 2020 Publication	<1 %
52	Shuping Zhang, Qing Dong, Tao Chen, Yuanquan Xiong. "Combination of Light Bio-oil Washing and Torrefaction Pretreatment of Rice Husk: Its Effects on Physicochemical Characteristics and Fast Pyrolysis Behavior", Energy & Fuels, 2016	<1 %

Publication

53	Xue, Zhong, Zhang, Xu. "Performance of Catalytic Fast Pyrolysis using a y-Al2O3 Catalyst with Compound Modification of ZrO2 and CeO2", Catalysts, 2019 Publication	<1 %
54	Xue-Yu Ren, Xiao-Bo Feng, Jing-Pei Cao, Wen Tang et al. "Catalytic Conversion of Coal and Biomass Volatiles: A Review", Energy & Fuels, 2020 Publication	<1 %
55	Yunwu Zheng, Jida Wang, Donghua Li, Can Liu, Yi Lu, Xu Lin, Zhifeng Zheng. "Highly efficient catalytic pyrolysis of biomass vapors upgraded into jet fuel range hydrocarbon-rich bio-oil over a bimetallic Pt–Ni/y-Al2O3 catalyst", International Journal of Hydrogen Energy, 2021 Publication	<1 %
56	mdpi-res.com Internet Source	<1 %
57	openprairie.sdstate.edu Internet Source	<1 %
58	pt.scribd.com Internet Source	<1 %
59	pubs.acs.org Internet Source	<1 %

60	tel.archives-ouvertes.fr Internet Source	<1 %
61	F. A. Agblevor, H. Wang, S. Beis, K. Christian, A. Slade, O. Hietsoi, D. M. Santosa. " Reformulated Red Mud: a Robust Catalyst for Catalytic Pyrolysis of Biomass ", Energy & Fuels, 2020 Publication	<1 %
62	Javier Remón, Marina Casales, Jesús Gracia, María S. Callén, José Luis Pinilla, Isabel Suelves. "Sustainable production of liquid biofuels and value-added platform chemicals by hydrodeoxygenation of lignocellulosic bio-oil over a carbon–neutral Mo2C/CNF catalyst", Chemical Engineering Journal, 2021 Publication	<1 %
63	Minghao Zhou, Jun Ye, Peng Liu, Junming Xu, Jianchun Jiang. "Water-Assisted Selective Hydrodeoxygenation of Guaiacol to Cyclohexanol over Supported Ni and Co Bimetallic Catalysts", ACS Sustainable Chemistry & Engineering, 2017 Publication	<1 %
64	Murtala M. Ambursa, Joon Ching Juan, Y. Yahaya, Y.H. Taufiq-Yap, Yu-Chuan Lin, Hwei Voon Lee. "A review on catalytic hydrodeoxygenation of lignin to transportation fuels by using nickel-based	<1 %

catalysts", Renewable and Sustainable Energy Reviews, 2021
Publication

---

65 Panya Maneechakr, Surachai Karnjanakom. "Improving the Bio-Oil Quality via Effective Pyrolysis/Deoxygenation of Palm Kernel Cake over a Metal (Cu, Ni, or Fe)-Doped Carbon Catalyst", ACS Omega, 2021 <1 %
Publication

---

66 Shinyoung Oh, Hyewon Hwang, Hang Seok Choi, Joon Weon Choi. "The effects of noble metal catalysts on the bio-oil quality during the hydrodeoxygenative upgrading process", Fuel, 2015 <1 %
Publication

---

67 Swathi Mukundan, Gandham Sriganesh, Pramod Kumar. "Upgrading Prosopis juliflora to biofuels via a two-step pyrolysis – Catalytic hydrodeoxygenation approach", Fuel, 2020 <1 %
Publication

---

68 Zhi-Cong Wang, Pei-Gao Duan, Xiao-Jie Liu, Feng Wang, Yu-Ping Xu. "Hydrotreating the Low-Boiling-Point Fraction of Biocrude in Hydrogen Donor Solvents for Production of Trace-Sulfur Liquid Fuel", Industrial & Engineering Chemistry Research, 2019 <1 %
Publication

---

69 gyan.iitg.ernet.in

	Internet Source	<1 %
70	ir.lib.uwo.ca Internet Source	<1 %
71	istina.ipmnet.ru Internet Source	<1 %
72	jlupub.ub.uni-giessen.de Internet Source	<1 %
73	par.nsf.gov Internet Source	<1 %
74	prism.ucalgary.ca Internet Source	<1 %
75	publikationen.bibliothek.kit.edu Internet Source	<1 %
76	repository.kaust.edu.sa Internet Source	<1 %
77	scholar.uwindsor.ca Internet Source	<1 %
78	www.doria.fi Internet Source	<1 %
79	www.research.manchester.ac.uk Internet Source	<1 %
80	www.tandfonline.com Internet Source	<1 %

81	Emmanuel Galiwango, Ali H. Al-Marzuoqi, Abbas A. Khaleel, Mahdi M. Abu-Omar. "Catalytic Depolymerization of Date Palm Waste to Valuable C5–C12 Compounds", Catalysts, 2021 Publication	<1 %
82	Qiang Deng, Jiawei Zhu, Yao Zhong, Xiang Li, Jun Wang, Jianxin Cai, Zheling Zeng, Ji-Jun Zou, Shuguang Deng. "MOF-Encapsulating Metal–Acid Interfaces for Efficient Catalytic Hydrogenolysis of Biomass-Derived Aromatic Aldehydes", ACS Sustainable Chemistry & Engineering, 2021 Publication	<1 %
83	Weiting Liao, Xin Wang, Lu Li, Di Fan, Zhiyu Wang, Yongqiang Chen, Yan Li, Xin'an Xie. "Catalytic Alcoholysis of Lignin with HY and ZSM-5 Zeolite Catalysts", Energy & Fuels, 2019 Publication	<1 %
84	"Production of Biofuels and Chemicals with Pyrolysis", Springer Science and Business Media LLC, 2020 Publication	<1 %
85	A N Pulungan, Nurfajriani, A Kembaren, J L Sihombing, C V Ginting, A Nurhamidah, R Hasibuan. "The stabilization of bio-oil as an alternative energy source through hydrodeoxygenation using Co and Co-Mo	<1 %

supported on active natural zeolite", Journal of Physics: Conference Series, 2022
Publication

---

86 Bojun Zhao, Yulin Hu, Jihui Gao, Guangbo Zhao, Madhumita B. Ray, Chunbao Charles Xu. "Recent Advances in Hydroliquefaction of Biomass for Bio-oil Production Using In Situ Hydrogen Donors", Industrial & Engineering Chemistry Research, 2020 <1 %
Publication

---

87 J L Sihombing, E Ginting, S Amdayani, A N Pulungan, V Tanjung, A A Sandy, R Rahayu. "Characterization of sarulla natural zeolite activated with various acid concentration and loaded with Ni and Ni-Mo metals as bifunctional catalysts", Journal of Physics: Conference Series, 2022 <1 %
Publication

---

88 Meena Marafi, Edward Furimsky. "Hydroprocessing Catalysts Containing Noble Metals: Deactivation, Regeneration, Metals Reclamation, and Environment and Safety", Energy & Fuels, 2017 <1 %
Publication

---

89 Mustafa Al-Sabawi, Jinwen Chen. "Hydroprocessing of Biomass-Derived Oils and Their Blends with Petroleum Feedstocks: A Review", Energy & Fuels, 2012 <1 %
Publication

90	Pooya Lahijani, Maedeh Mohammadi, Abdul Rahman Mohamed, Farzad Ismail, Keat Teong Lee, Ghazaleh Amini. "Upgrading biomass-derived pyrolysis bio-oil to bio-jet fuel through catalytic cracking and hydrodeoxygenation: A review of recent progress", Energy Conversion and Management, 2022 Publication	<1%
91	R. Mallada, M. Menéndez, J. Santamaŕıa. "On the favourable effect of CO2 addition in the oxidation of butane to maleic anhydride using membrane reactors", Applied Catalysis A: General, 2002 Publication	<1%

Exclude quotes	On	Exclude matches	Off
Exclude bibliography	On		